Biotechnology Journal
www.biotechnology-journal.com

Extruded Bioreactor Perfusion Culture Supports the Chondrogenic Differentiation of Human Mesenchymal Stem/Stromal Cells in 3D Porous Poly(ε-Caprolactone) Scaffolds

*João C. Silva, Carla S. Moura, Gonçalo Borrecho, António P. Alves de Matos, Cláudia L. da Silva, Joaquim M. S. Cabral, Paulo J. Bártolo, Robert J. Linhardt, and Frederico Castelo Ferreira**

Novel bioengineering strategies for the ex vivo fabrication of native-like tissue-engineered cartilage are crucial for the translation of these approaches to clinically manage highly prevalent and debilitating joint diseases. Bioreactors that provide different biophysical stimuli have been used in tissue engineering approaches aimed at enhancing the quality of the cartilage tissue generated. However, such systems are often highly complex, expensive, and not very versatile. In the current study, a novel, cost-effective, and customizable perfusion bioreactor totally fabricated by additive manufacturing (AM) is proposed for the study of the effect of fluid flow on the chondrogenic differentiation of human bone-marrow mesenchymal stem/stromal cells (hBMSCs) in 3D porous poly(ε-caprolactone) (PCL) scaffolds. hBMSCs are first seeded and grown on PCL scaffolds and hBMSC–PCL constructs are then transferred to 3D-extruded bioreactors for continuous perfusion culture under chondrogenic inductive conditions. Perfused constructs show similar cell metabolic activity and significantly higher sulfated glycosaminoglycan production (≈1.8-fold) in comparison to their non-perfused counterparts. Importantly, perfusion bioreactor culture significantly promoted the expression of chondrogenic marker genes while downregulating hypertrophy. This work highlights the potential of customizable AM platforms for the development of novel personalized repair strategies and more reliable in vitro models with a wide range of applications.

1. Introduction

Cartilage self-repair occurring upon injury or degenerative joint disease such as osteoarthritis or rheumatoid arthritis is hampered by the intrinsic avascular nature and low cellularity of this tissue. Appropriate therapeutic strategies to regenerate cartilage with properties similar to the native tissue and with long-term functionality have yet to be developed.[1,2] Cartilage tissue engineering (CTE) approaches, aiming at fabricating tissue substitutes that recapitulate the biochemical, structural, and mechanical properties of native cartilage, have been introduced as promising alternatives to current clinical surgical methods.[3] Such strategies often comprise a combination of cells (chondrocytes or mesenchymal stem/stromal cells [MSCs]), biomaterial scaffolds, and external stimuli through the modulation of biological and/or physical factors.[3–5]

MSCs have been used in CTE as an attractive alternative to chondrocytes due to the easier accessibility of these cells from a wide variety of tissue sources; MSCs' higher

Dr. J. C. Silva, Prof. C. L. da Silva, Prof. J. M. S. Cabral, Prof. F. C. Ferreira
Department of Bioengineering and iBB - Institute of Bioengineering and Biosciences
Instituto Superior Técnico
Universidade de Lisboa
Av. Rovisco Pais, Lisboa 1049-001, Portugal
E-mail: frederico.ferreira@tecnico.ulisboa.pt
Dr. J. C. Silva, Prof. R. J. Linhardt
Department of Chemistry and Chemical Biology, Biological Sciences, Biomedical Engineering and Chemical and Biological Engineering
Center for Biotechnology and Interdisciplinary Studies
Rensselaer Polytechnic Institute
Troy, NY 12180-3590, USA
The ORCID identification number(s) for the author(s) of this article can be found under https://doi.org/10.1002/biot.201900078

DOI: 10.1002/biot.201900078

Dr. C. S. Moura
CDRSP – Centre for Rapid and Sustainable Product Development
Polytechnic Institute of Leiria
Rua de Portugal-Zona Industrial, Marinha Grande 2430-028, Portugal
G. Borrecho, Prof. A. P. A. de Matos
Centro de Investigação Interdisciplinar Egas Moniz (CiiEM)
Quinta da Granja
Monte da Caparica, 2829-511 Caparica, Portugal
Prof. P. J. Bártolo
School of Mechanical and Aerospace and Civil Engineering
University of Manchester
Oxford Road, Manchester M13 9PL, UK

in vitro proliferative potential and immunomodulatory/trophic properties; and ability to differentiate toward cartilage upon induction with proper external cues.[2,6,7]

Biodegradable scaffold matrices based either on naturally occurring or synthetic materials have been widely used in combination with MSCs for CTE strategies.[8] Natural materials offer advantages such as low toxicity and presence of biological signaling and cell adhesion motifs, however, batch-to-batch variability, weak mechanical properties, and difficulty in controlling structure and degradation are important drawbacks to consider. In contrast, the main benefits of using synthetic scaffolds reside in the good mechanical support provided, ease of processing, and the possibility of controlling the mechanical properties and degradation times by changing the polymer chemical structure or scaffold architecture.[4,8,9] Among synthetic materials, poly(ε-caprolactone) (PCL), which was previously approved by the FDA for various medical applications, has been used as scaffold material with MSCs in different cartilage repair settings[10–12] mainly due to its biodegradability, chemical versatility, facile processability, and capacity to tune its mechanical properties to meet the requirements of a specific tissue engineering approach.[13,14]

Integrated CTE approaches have also employed the use of external cues to augment MSC chondrogenic potential. Such signaling cues can be biochemical (e.g., growth factors, TGF-β superfamily, fibroblast growth factor (FGF)-2,[15,16] or small molecules such as kartogenin[17]), environmental (e.g., low oxygen concentrations compared to atmospheric air, hypoxia, to recapitulate the in vivo oxygen tensions of articular cartilage (1% O_2 in the deep zone to 6% O_2 in the superficial zone) as well as of most MSC niches (1–5% O_2)[18–20] or physical factors (e.g., mechanical/electrical stimulation).[21,22] In fact, low oxygen tension culture conditions (generally between 3% and 5% O_2) have been employed to enhance MSC chondrogenesis in porous CTE scaffolds.[23,24] Bioreactor technology has been successfully employed for the expansion of MSC[25] and/or for chondrogenic priming,[26] prior to tissue substitute fabrication. In CTE strategies, commercially and tailor-made bioreactor devices have been developed, to apply controlled and dynamic mechanical stimuli to cell-seeded scaffolds aiming to generate cartilage-like tissue in vitro by a closer mimicking of the articular motion forces.[22,27] Examples of mechanical loading applied through bioreactor platforms to regulate MSC chondrogenic differentiation in CTE settings include direct compression,[28,29] hydrostatic pressure,[30] direct shear stress,[31] fluid-induced shear stress,[32–34] or multimodal biaxial combining different stimuli.[35,36] Such bioreactor platforms are often complex systems designed to meet specific requirements for a standardized scaffold structure and biophysical stimuli. A lack of versatility represents a major drawback for the generalized use of bioreactors in personalized CTE strategies, as any modification of the standardized bioreactor often requires costly and laborious manufacturing steps.[37,38] Additive manufacturing (AM) technology, such as 3D melt-extrusion, offers a promising alternative to overcome these limitations allowing the versatile and cost-effective fabrication of both scaffold and bioreactor with the desired size, shape, and architecture complexity.[39] Notably, this highly reproducible and flexible approach is fully compliant with a personalized CTE approach as the "patient-tailored" scaffold can be produced to perfectly fit the defect site and bioreactor prototypes can be easily customized to provide the specific physical stimuli required for each case.

Fluid perfusion within the constructs allows an efficient nutrient/metabolite transfer and gas exchange beneficial for cartilage extracellular matrix (ECM) synthesis. Additionally, previously published literature suggest that shear stress, resulting from fluid perfusion, favors the chondrogenic differentiation of MSCs.[32,33] Nevertheless, reports on hypertrophy observed in MSC-based cartilage engineered tissues under perfused culture[34] highlight the need for further studies to better understand the effects of fluid-induced shear stress in MSC chondrogenesis and thus optimize its application in CTE approaches.

In this study, we propose a new concept of a cost-effective and customizable perfusion bioreactor, readily fabricated by AM 3D-extrusion, to study the effect of fluid-induced shear stress on the chondrogenic differentiation of human bone marrow MSCs (hBMSCs) in porous PCL scaffolds. Unlike the majority of previous designs, the bioreactor presented here is totally produced by extrusion using standard and commercially available 3D printer and low-cost materials, without the need for additional complex metallic pieces, which allows its widespread use in clinical applications or for academic research purposes. Extruded bioreactor dimensions and perfusion system were conceptualized to allow for the use of several bioreactors in parallel, easily fitted on standard incubator chambers and perfused using a multichannel peristaltic pump. Moreover, this bioreactor platform can easily accommodate multiple scaffolds receiving uniform fluid-flow induced shear stress stimuli simultaneously and allows the simple collection of the engineered tissue constructs, in contrast to other designs requiring a more time-consuming and cumbersome handling.[33,40] Importantly, these devices can be easily modified to receive as many scaffolds as required, with different sizes and shapes according to the patient lesion site. This extruded bioreactor system explores the use of fluid-flow induced shear stress as a single mechanical stimuli to improve the quality of MSC-based cartilage tissue-engineered constructs. Herein, computer-aided design (CAD) models of the bioreactor prototypes were used for fluid-flow modeling. The perfusion system introduced here significantly enhanced the chondrogenic potential of hBMSC, while preventing tissue hypertrophy, as demonstrated by the results of sulfated glycosaminoglycan (sGAG) production, and immunohistochemical and gene expression analysis when compared with cells cultured under static culture conditions.

2. Experimental Section

2.1. Cell Isolation and Culture

hBMSCs were isolated from bone marrow (BM) aspirates (two male donors: 35 and 36 years of age) according to a previously established protocol.[41] BM samples were obtained from healthy donors upon informed consent, with the approval of the Ethics Committee of Instituto Português de Oncologia Francisco Gentil. Isolated hBMSCs were cultured using low-glucose DMEM

(Gibco, Thermo Fisher Scientific, MA, USA) supplemented with 10% v/v fetal bovine serum MSC-qualified (FBS; Life Technologies, CA, USA) and 1% v/v antibiotic-antimycotic (Anti-Anti, Gibco), kept at 37 °C and 5% CO_2 in humidified atmosphere and cryopreserved in a liquid/vapor-phase nitrogen container until further use. All the experiments were performed using cells between passages P3 and P5, and culture media was fully replaced every 3–4 days.

2.2. Fabrication and Characterization of PCL Scaffolds

PCL (MW 50 000 Da, CAPA 6500, Perstorp Caprolactones, UK) scaffolds were fabricated using in-house developed melt-extrusion equipment, the Bioextruder, and characterized as previously described.[42,43] Scaffolds were fabricated with the desired size (dimensions: 10 mm × 10 mm × 3 mm) and with a selected 0–90° lay-down pattern according to previously designed 3D CAD models (*SolidWorks* software, Dassault Systèmes, S.A., France). The produced scaffolds were characterized in terms of structure and architectural features by scanning electron microscopy (SEM, Hitachi S-2400, Japan) and micro-computed tomography (μ-CT, Scansky 1174v2, Bruker version 1.1, MA, USA). During the μ-CT analysis, the 3D image reconstruction was done in the software NRecon (version 1.7.0.4, Bruker) and the morphological features assessment was performed using the CT-Analyzer software (CTAn, version 1.16.4.1, Bruker). The porosity of the fabricated PCL scaffolds was calculated as the ratio between the pore volume and the sum of whole volume including pores and scaffold fibers (Porosity (%) = $(V_{pores}/(V_{pores} + V_{scaffold})) \times 100$). The scaffold's interconnectivity corresponds to the ratio between the volume of interconnected (or open) pores and the sum of the interconnected and closed pores (Interconnectivity (%) = $(V_{open\ pores}/(V_{open\ pores} + V_{close\ pores})) \times 100$).

2.3. Design and Fabrication of Extruded Perfusion Bioreactors

The bioreactor prototype parts were generated employing CAD (*SolidWorks* software) and fabricated by melt-extrusion using a commercially available 3D printer (MakerBot Replicator 2X, MakerBot Industries, NY, USA). The parts of the cylindrical shape bioreactor were produced in acrylonitrile butadiene styrene (ABS, MakerBot) using the fabrication parameters described in **Figure 1**B(iii). Three individual parts composing the bioreactor were extruded: an external vase, an internal part able to perfectly fit the PCL scaffolds, and a lid that can assemble a 25 cm^2 t-flask lid with a filter (Corning Inc., NY, USA) to allow oxygenation (Figure 1B(i),(ii)). The bioreactor vessel was designed to fit six PCL scaffolds and with a working volume of 25 mL of culture media. The outer bioreactor surfaces were coated with a thin layer of poly (dimethylsiloxane) (PDMS; SYLGARD 184 Silicone Elastomer Kit, Corning Inc.) to seal any porosity and prevent media leakage. Additionally, the bioreactor vessel was connected to a peristaltic pump (Ismatec REGLO digital peristaltic pump, Ismatec, Germany) through Tygon tubes (Ismatec) to allow for controlled perfusion with culture media. The fluid flows in a closed system from the bottom left (inlet) of the bioreactor and leaves the reactor vessel by the top right (outlet) (Figure 3B).

2.4. Computational Fluid Dynamic Analysis

A computational fluid dynamics (CFD) simulation was performed using the *ANSYSWorkbench* 2.0 Framework software (version R19.1, ANSYS Inc., PA, USA) to predict the fluid velocities in different regions within the bioreactor vessel. The conditions for the computational simulations were defined as: bioreactor working volume, 25 mL; flow rate, 0.2 mL min^{-1} (as used in the in vitro culture experiments); temperature, 37 °C; pressure of 1 atm; and flow regime defined as subsonic and turbulence model as laminar. The pressure at the bioreactor vessel outlet was assumed to be zero and the bioreactor chamber was considered as rigid and impermeable.

2.5. In Vitro Cytotoxicity Testing of the Materials Comprising the Bioreactor Platform

The biocompatibility of the ABS material used in the bioreactor (discs with 10 mm diameter and 2 mm thickness produced with different printing infills: 25%, 50%, 75%, and 100%) as well as the PCL scaffold was tested following the ISO 10 993–5 guidelines[44] using L929 mouse fibroblasts (ATCC number CCL-1). All materials were evaluated by the indirect extract test and direct contact test. Cells cultured on tissue culture polystyrene (TCPS) plates with DMEM + 10% FBS + 1% Anti-Anti culture medium under standard conditions were used as negative control and latex was used as positive control for cell death. Extracts were prepared by incubating the materials in culture media (0.2 g material mL^{-1}) for 72 h at 37 °C and 5% CO_2 under agitation. To perform both tests, L929 fibroblasts were seeded on TCPS plates at a cell density of 1.5×10^5 cells per well and cultured for 24 h at 37 °C and 5% CO_2 to obtain a confluent monolayer. Culture media was removed and cells were exposed to the extract's conditioned medium for 24 h at 37 °C and 5% CO_2 for the indirect extract test. Afterward, extract conditioned medium was removed and the MTT assay (In Vitro Toxicology Assay Kit, MTT based, Sigma–Aldrich, MO, USA) was performed according to the manufacturer's guidelines. Briefly, cells were incubated with MTT solution (yellow, 1 mg mL^{-1}) for 2 h at 37 °C; and the violet formazan product (resultant from the MTT metabolic reduction by metabolically active cells) dissolved using a 0.1 N HCl solution in anhydrous isopropanol (Sigma–Aldrich). The absorbance of the resultant solution was measured in a plate reader (Infinite M200 PRO, TECAN, Switzerland) at 570 nm, and the percentage of viable cells for the different samples was calculated by comparison with the values obtained for the negative control cultures. Three samples of each condition were assayed and the absorbance of each sample was measured in triplicate. In the direct contact test, the different materials were placed in contact with a confluent monolayer of L929 fibroblasts and incubated for 24 h at 37 °C and 5% CO_2. Cell viability and morphology were qualitatively assessed under an inverted optical microscope (LEICA DMI3000B, Leica Microsystems, Germany) equipped with a digital camera (Nikon DXM1200F, Nikon Instruments Inc., Japan).

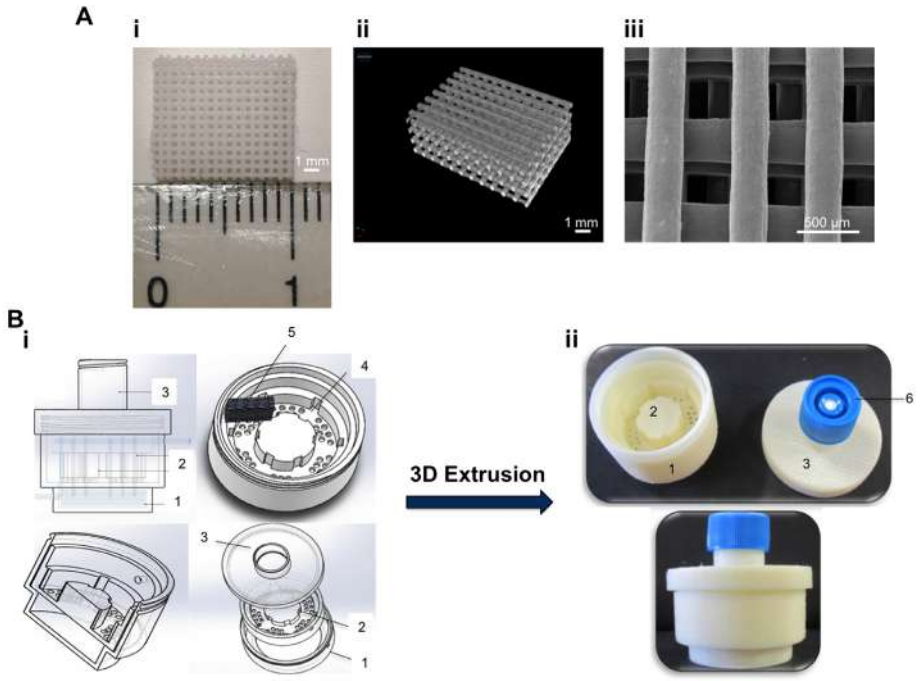

iii Bioreactor fabrication parameters:

Material	Acrylonitrile butadiene styrene (ABS)
Printing infill	100%
Layer height	0.2 mm
Extrusion head temperature	230°C
Build plate temperature	110°C
Speed while extruding	50 mm/s
Bioreactor mass	39.4 g
Working volume	25 mL
# scaffold compartments	6

Figure 1. Fabrication of PCL scaffold and extruded bioreactor platform. A) Characterization of 3D extruded PCL scaffolds structure: photograph of a PCL scaffold with 10 mm × 10 mm × 3 mm dimensions (i), respective 3D reconstruction image obtained after µ-CT analysis (ii) and SEM micrograph (iii). Scale bar: 1 mm for (i) and (ii), and 500 µm for (iii). B) CAD models of the parts composing the bioreactor prototype (i) were developed using *SolidWorks* software. The bioreactor consists of an external vase (1), an internal part (2) with a bottom porous disperser and a scaffold chamber including compartments (4) to perfectly fit six PCL scaffolds (5), and a lid (3) designed to assemble a filter t-flask cap (6) to allow oxygenation. Both internal and external vases have holes to allow connection to a peristaltic pump through tubing and the bottom of the internal vase possesses a porous disperser to allow fluid movement. Fluid flows in a closed system, entering the bioreactor from the bottom left (inlet), and leaves the vessel by the top right (outlet). Prior to whole bioreactor assembly, the parts were fabricated in ABS material by 3D melt-extrusion (ii) using defined printing parameters (iii).

2.6. Bioreactor Culture of hBMSC–PCL Constructs

PCL scaffolds were sterilized by UV exposure (2 h each side of the scaffold) and by incubation in 70% v/v ethanol for 3 h. The scaffolds were washed three times with a 1% v/v Anti-Anti solution in phosphate buffered saline (PBS, Gibco) for 3 h (1 h each wash) and conditioned with culture media for 1 h at 37 °C. Each PCL scaffold placed on TCPS plates was seeded with 1.5×10^5 hBMSCs and incubated for 1.5 h at 37 °C and 5% CO_2, before being completely immersed with culture media, to promote initial cell attachment. hBMSCs were expanded in PCL scaffolds for 14 days in DMEM + 10% FBS + 1% Anti-Anti at 37 °C/5% CO_2/20% O_2 and the culture media was fully renewed twice a week. During this period, hBMSCs spread on the extruded PCL fibers and migrate along the whole structure, occupying both fibers and pore regions of the scaffold.[45] Before the dynamic/static culture of hBMSC–PCL constructs, bioreactors and tubes were sterilized thoroughly by 70% ethanol and 1% Anti-Anti (in PBS) washing. At day 14, hBMSC–PCL constructs were transferred to the bioreactor prototypes and cultured under perfusion (volumetric flow rate of 0.2 mL min^{-1}, based on previously reported studies[33,46]) or static conditions with 25 mL of chondrogenic medium (Hyclone AdvanceSTEM Chondrogenic Differentiation medium, Thermo Scientific, Rockford, IL USA) + 1% Anti-Anti for additional 21 days. All bioreactor cultures were performed at 37 °C/5% CO_2 under hypoxic conditions (5% O_2 tension) to generate closer mimicry of the in vivo articular cartilage microenvironment and to promote MSC chondrogenic differentiation. For a single experiment, each bioreactor (static/perfused) harbored six different hBMSC–PCL constructs and 50% of the culture media was replaced weekly.

2.7. hBMSC Viability and Proliferation Assay

The viability and proliferation of hBMSC in PCL scaffolds were evaluated throughout the 5 weeks of culture (days 1, 7, 14, 21, 28, and 35) by assessing cell metabolic activity using AlamarBlue cell viability reagent (ThermoFisher Scientific, USA) according to the manufacturer's protocol. In this assay, the scaffolds were removed from the bioreactors and placed in a multi-well plate. AlamarBlue cell viability reagent was diluted in culture media (1:10 dilution, v/v), added to the scaffolds and incubated at 37 °C in a 5% CO_2 chamber for 2.5 h. For each independent experiment, fluorescence intensity values were quantified in triplicate using a plate reader (Infinite M200 PRO, TECAN) at 560/590 nm excitation/emission wavelengths and compared to a calibration curve (specific for each donor) to estimate the equivalent number of cells in the scaffolds. Acellular PCL scaffolds were used as blank control for the fluorescence intensity measurements.

2.8. Metabolite Analysis

The concentrations of glucose and lactate were analyzed before and after each media change during the culture of hBMSC under static conditions in PCL scaffolds and hBMSC–PCL constructs in the bioreactor. The collected media samples were centrifuged for 10 min to remove dead cells and debris. Metabolite concentrations were determined using an automatic multi-parameter analyzer (YSI 7100MBS, Yellow Springs Instruments, OH, USA). Specific glucose consumption rate, specific lactate production rate, and the apparent yield of lactate from glucose ($Y_{Lac/Gluc}$) for defined culture time intervals during hBMSC expansion and chondrogenic differentiation were calculated according to a previously published method.[41]

2.9. Assessment of hBMSC Chondrogenic Differentiation

2.9.1. sGAG detection and Quantification Assay

At the end of the bioreactor culture (day 35), scaffold samples were harvested, washed thoroughly with PBS to remove all media remnants, and fixed with 2% paraformaldehyde (PFA, Sigma–Aldrich) solution for 20 min. Samples were incubated with 1% Alcian Blue 8GX (Sigma–Aldrich) solution (in 0.1 N hydrochloric acid) for 1 h to assess for the presence of sGAG. Scaffold constructs were rinsed twice with PBS, washed once with distilled water and imaged using an inverted microscope (LEICA DMI3000B, Leica Microsystems) equipped with a digital camera (Nikon DXM1200F, Nikon Instruments Inc.). sGAG content of the final tissue constructs was quantified by Alcian Blue dye precipitation following previously reported protocols.[47,48] In this assay, Alcian Blue stained samples were re-dissolved with a 2% SDS (Sigma–Aldrich) solution with constant agitation overnight. Absorbance values of the resultant solutions were quantified in a plate reader (Infinite M200 PRO, TECAN) at 620 nm and compared to a calibration curve to estimate the sGAG content in each construct. In each independent experiment, three scaffolds per experimental group were considered and the absorbance of each sample was measured in triplicate. Acellular PCL scaffolds submitted to the same protocol were used as blank control for the absorbance measurements.

2.9.2. Histological and Immunohistochemical Analysis

The final tissue constructs obtained after the bioreactor culture were harvested, rinsed with PBS, and fixed in 2% PFA. The samples were dehydrated with a progressive graded ethanol series, cleared with xylene (Sigma–Aldrich) and embedded in paraffin. The paraffin blocks were sliced into 5 µm sections using a microtome Leica RM2235 (Leica Biosystems) and mounted in glass slides. Upon deparaffinization and rehydration of the slides, endogenous peroxidase activity was blocked with 3% v/v hydrogen peroxidase (H_2O_2, Sigma–Aldrich) treatment for 10 min. For histological evaluation of the constructs, the cross-sections were stained with haematoxylin–eosin (H&E, Sigma–Aldrich) for 5 min to visualize cells or cell nuclei; 0.1% w/v Toluidine Blue (Sigma–Aldrich) for 5 min to identify proteoglycans; and with 1% w/v Safranin-O (Sigma–Aldrich) for 15 min to observe secreted GAG. In the immunohistochemical analysis, cross-sections were incubated overnight at room temperature with rabbit polyclonal antibodies to collagen II (1:800 dilution, Anti-Collagen II antibody ab34712, Abcam, UK) and aggrecan (1:250 dilution, Anti-Aggrecan II antibody ab140707, Abcam), followed by incubation for 30 min with anti-rabbit Dako EnVision$^+$ System-HRP Labeled Polymer (Agilent Dako, CA, USA). Slides were counterstained with haematoxylin, dehydrated, and mounted. Images of the histological and immunohistochemical stainings were obtained at 200× magnification using a Leica DMLB optical microscope equipped with a Leica DFC290 HD camera (Leica Microsystems).

2.9.3. RNA Extraction and Quantitative Real-Time PCR Analysis

Scaffolds were collected and kept at –80 °C until further analysis to quantify the expression of chondrogenic gene markers by cells at the end of perfusion/non-perfusion bioreactor culture. Total RNA was isolated using the RNeasy Mini Kit (Qiagen, Hilden, Germany). The scaffolds were first incubated in lysis buffer with agitation for 20 min at 4 °C, followed by the total RNA extraction protocol according to the manufacturer's guidelines. RNA was quantified by UV spectrophotometry (NanoVue Plus, GE Healthcare, Chicago, IL, USA). cDNA was synthesized from the purified RNA using iScript cDNA Synthesis Kit (Bio-Rad, Hercules, CA, USA) and the T100 Thermal Cycler (Bio-Rad) following the manufacturer's supplied protocol. The quantitative real-time PCR (qPCR) analysis was performed using Fast SYBR Green Master Mix (Applied Biosystems, CA, USA) and a StepOne Real-Time PCR System (Applied Biosystems) according to the manufacturer's guidelines. The primer sequences (Stabvida, Portugal) used in the qPCR analysis are specified in Table S1, Supporting Information. All samples were assayed in triplicate and the CT values obtained were normalized against the expression of the housekeeping gene glyceraldehyde-3-phosphate dehydrogenase (*GAPDH*). The analysis was performed using the $2^{-\Delta\Delta CT}$ method, and data were presented as fold-change expression levels relative to hBMSCs at day 0.

2.10. Statistical Analysis

Results are presented as mean ± standard error of mean (SEM) of the values obtained for three ($n = 3$) independent experiments, unless otherwise specified. Statistical analysis was performed using GraphPad Prism 6.0 software (GraphPad Software Inc., La Jolla, USA). Comparisons between independent samples (perfusion bioreactor vs non-perfusion bioreactor) were determined by the nonparametric Mann–Whitney *U* test and data were considered to be statistically significant when *p*-values obtained were <5% ($^{*}p < 0.05$).

3. Results

3.1. Design and Fabrication of PCL Scaffolds and Perfusion Bioreactor Platform

PCL scaffolds (Figure 1A(i)) were produced in a controlled layer-by-layer process using an AM 3D-extrusion system developed in-house, and with the desired shape, size, and architecture.[43] The structural features of the fabricated scaffolds were assessed by μ-CT (Figure 1A(ii)) and SEM (Figure 1A(iii)) analysis. Scaffolds with a 0–90° fiber orientation and a pore size of 390 μm that falls within the range of pore sizes previously reported to promote MSC chondrogenesis[49,50] were generated to achieve high porosity (56.6%) and high interconnectivity (99.7%),[43] which favor cell infiltration and migration, efficient gas exchange, nutrient supply, and waste removal.

Bioreactor prototypes were fabricated from the designed CAD models (Figure 1B(i)) using a commercially available 3D extrusion system. As demonstrated in Figure 1B, three parts extruded independently were assembled to compose the whole bioreactor (Figure 1B(ii)): an external vase, an inner part customized to perfectly accommodate the PCL scaffolds, and a lid that can harbor a vented t-flask cap. The prototype was developed to allow fluid perfusion of the scaffolds inside the bioreactor by connection through tubing to a peristaltic pump. Culture media enter the bioreactor vessel from the bottom left part (inlet), flow through a thin chamber on the bottom of the reactor, and then upstream, through a porous disperser in the bottom surface of the bioreactor into the scaffolds chamber. Then, the culture media exit the system from the top right (outlet). Additionally, based on this concept, the bioreactor was custom-made to accommodate six PCL scaffolds with a working volume of 25 mL using the extrusion parameters summarized in Figure 1B(iii).

Prior to cell culture experiments, the materials (ABS disks with different printing infill and PCL scaffolds) were tested for cytotoxicity using L929 fibroblasts following ISO 10 993–5 guidelines (Figure S1, Supporting Information). The MTT extract indirect test (Figure S1A, Supporting Information) showed that cells cultured with the extracts obtained from culture incubation of the different materials presented high cell viabilities over 86%, while cells cultured in direct contact with the same materials presented regular fibroblast morphology with no evidence of any inhibition halo effect or cell death (Figure S1B, Supporting Information).

3.2. CFD Analysis Predicts Fluid Velocities Distribution Within the Bioreactor

CFD modeling was used to simulate the flow pattern of the culture media within the extruded perfusion bioreactor vessel (**Figure 2**; Figure S2, Supporting Information). Before the analysis, a CAD model of the volume geometry of the bioreactor was imported from *SolidWorks* and a respective mesh was created in *ANSYS*. For the perfusion flow rate defined for the in vitro culture assays (0.2 mL min^{-1}), a residential time (time needed for the total replacement of the working volume in the bioreactor vessel) of 125 min (≈2.08 h) was estimated. Figure 2C shows the predicted fluid velocity distributions and values along six different horizontal planes inside the bioreactor vessel: a top plane near the outlet right above the scaffolds (1), three planes intersecting the scaffolds (2-4), a plane at the top surface of the bottom porous fluid disperser (5), and a plane at the lower surface of the bottom porous fluid disperser (6). In this configuration, the maximum linear velocities were observed near the inlet and outlet of the bioreactor, with an estimated value of $\approx 1.22 \times 10^{-5}$ m s^{-1}. The observation of the three planes (2–4) intersecting the scaffold compartments suggests that the fluid velocity distributions are quite homogeneous for all the six scaffolds. Moreover, this analysis indicates that the tangential fluid velocity values experienced by the scaffolds are quite low, which were previously hypothesized to favor chondrogenic phenotype maintenance.[51,52] The fluid perfusion through the bottom fluid disperser pores (plane 6 to 5) increased fluid velocities in the parallel regions between two adjacent scaffold compartments. Importantly, as shown in Figures 2A,B and 1B(i), the disperser was designed with no pores in the regions below the scaffold compartments to avoid the occurrence of high fluid velocities that may induce harmful or unwanted mechanical effects on the cell-scaffold constructs. An additional CFD analysis, predicting the fluid-flow velocity patterns and intensities in three different horizontal (Figure S2A(i–iv), Supporting Information) and vertical (Figure S2B(i–iv), Supporting Information) planes, is also provided. Overall, our simulation results demonstrate homogeneous fluid perfusion in the regions tangential to the scaffolds, suggesting uniform hydrodynamic stress conditions at the scaffold interface.

3.3. Bioreactor Culture of hBMSC–PCL Constructs

The in vitro assays for bioreactor culture were performed following the experimental scheme presented in **Figure** 3A. hBMSCs were expanded in PCL scaffolds for 2 weeks under static culture conditions in DMEM + 10% FBS + 1% Anti-Anti, and afterward, the hBMSC–PCL constructs were transferred to the ABS extruded perfusion bioreactors and cultured with a 0.2 mL min^{-1} flow rate of chondrogenic medium at 37 °C/5% CO_2/5% O_2 (Figure 3A,B). A bioreactor culture operating without perfusion was used as a control. The metabolic activity of the cells present in the PCL scaffolds monitored by AlamarBlue cell viability assay throughout culture are presented in Figure 3C. As expected, cell metabolic activities increased considerably during the first 14 days of culture in DMEM + 10% FBS + 1% Anti-Anti and were maintained during the following 21 days under chondrogenic

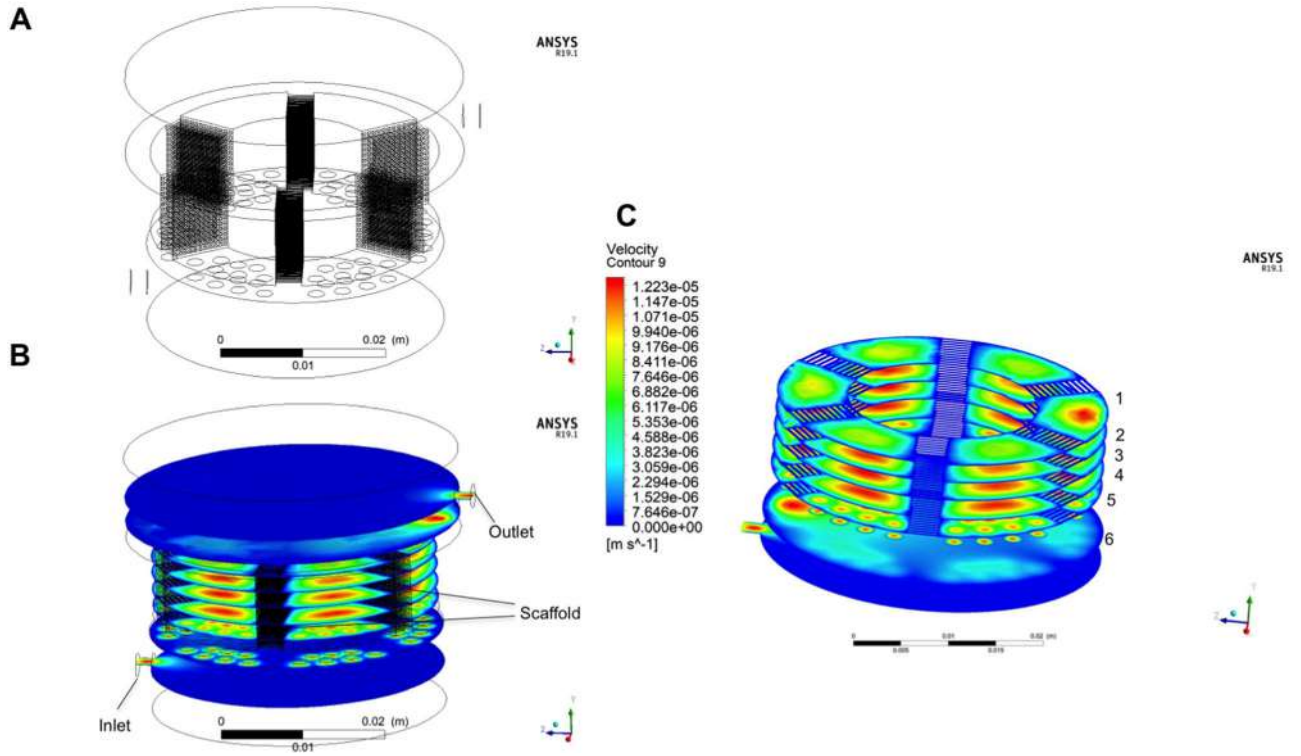

Figure 2. Computational fluid flow modeling predicts linear velocities distribution within the bioreactor. A) Representative model of the bioreactor inner region considered in the CFD analysis, specifying the location of the PCL scaffolds. B) Contour plot with the linear fluid velocities distribution inside the bioreactor, highlighting the inlet and outlet regions of the system. C) Fluid velocity distributions and values for linear velocities (expressed in m/s) for different horizontal planes (corresponding to different regions – a top plane near the outlet right above the scaffolds (1), three planes intersecting the scaffolds (2–4), a plane at the top surface of the bottom porous fluid disperser (5), and a plane at the lower surface of the bottom porous fluid disperser (6) within the bioreactor vessel. CFD analysis was performed using *ANSYS* software version R19.1 with the following parameters: 25 mL fluid volume in the bioreactor vessel; fluid perfusion rate of 0.2 mL min^{-1}; ambient conditions of 37 °C and 1 atm; flow regime defined as subsonic and turbulence model as laminar. The pressure at the bioreactor vessel outlet was assumed to be zero and the bioreactor chamber was considered as rigid and impermeable.

induction. Additionally, cells remained viable without significant differences in metabolic activity between non-perfusion and perfusion cultures in the bioreactor.

The concentrations of glucose (Figure 3D(i)) and lactate (Figure 3D(ii)) in the cell culture supernatants were measured to evaluate the cell metabolic profile throughout all culture periods (in static expansion and bioreactor differentiation stage). As expected, for both non-perfused/perfused bioreactors, glucose concentration decreased between each media change while lactate concentration showed an opposite trend. Additionally, under both conditions tested and throughout all culture time, glucose was always available (never reaching values close to 0 mM), while lactate concentration never reached inhibitory values (over 35 mM previously defined for human MSC[53]), with maximum values of 10.45 ± 0.07 mM and 11.75 ± 0.21 mM, observed at day 35 for bioreactor culture under static conditions and perfusion, respectively. Glucose consumption, lactate production and apparent yield of lactate from glucose throughout all culture experiments were calculated and are presented in Figure S3, Supporting Information. Under both conditions, a higher glucose specific consumption rate (Figure S3A, Supporting Information) and lactate specific production rate (Figure S3B, Supporting Information) were observed during the expansion phase under static conditions. From day 14 onward, the glucose specific consumption rate and lactate specific production rate values were considerably reduced, suggesting a lower cell metabolism during chondrogenic differentiation in bioreactor cultures under non-perfusion and perfusion conditions. Moreover, $Y_{Lac/Gluc}$ (Figure S3C, Supporting Information) during all culture stages (expansion and chondrogenic differentiation) were also calculated, ranging from 1.61 ± 0.07 to 3.19 ± 0.19 for non-perfused culture in the bioreactor (average $Y_{Lac/Gluc}$ = 2.37 during expansion; average $Y_{Lac/Gluc}$ = 2.51 during differentiation; and average $Y_{Lac/Gluc}$ = 2.45 for all culture) and 1.48 ± 0.04 to 2.94 ± 0.04 for perfusion bioreactor condition (average $Y_{Lac/Gluc}$ = 2.23 during expansion; average $Y_{Lac/Gluc}$ = 2.52 during differentiation; and average $Y_{Lac/Gluc}$ = 2.39 for all culture).

3.4. Perfusion Culture Enhances Cartilage ECM Production

At the end of bioreactor culture, the generated constructs were harvested and were assessed for the presence of typical cartilage ECM components. Both tissue constructs obtained after static or perfused bioreactor culture stained positively for

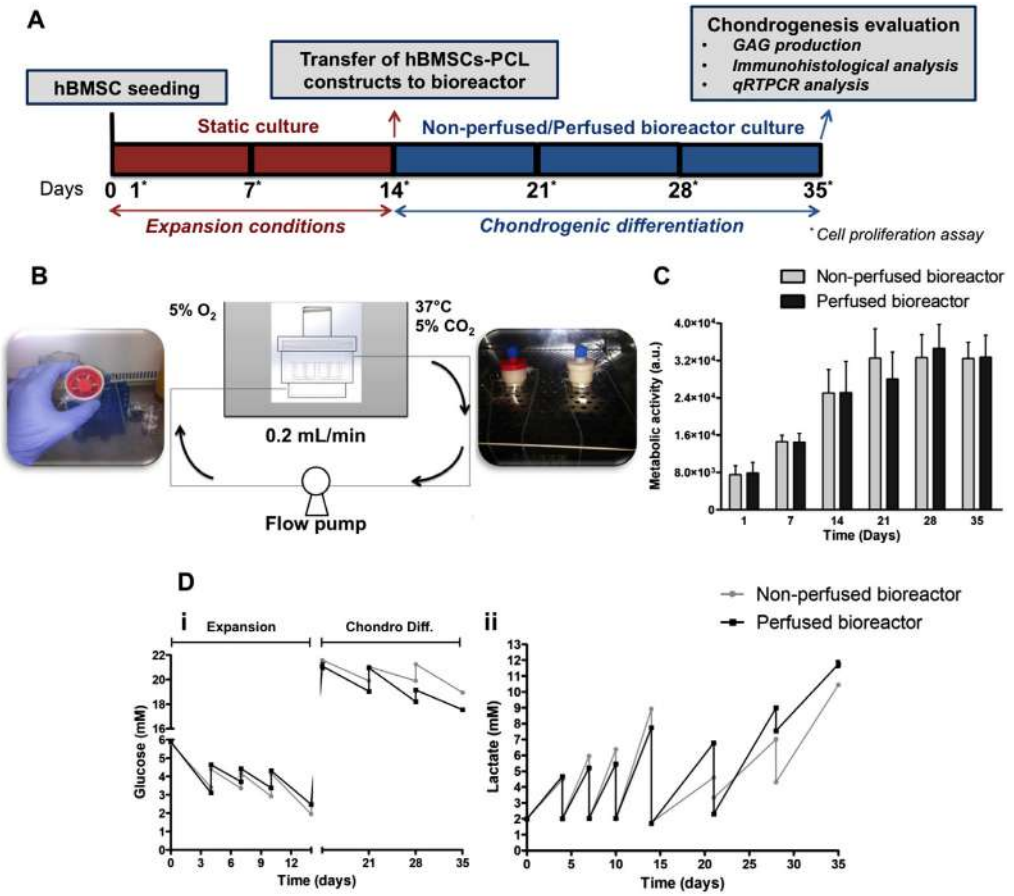

Figure 3. Bioreactor culture of hBMSC–PCL constructs. A) Scheme of the experimental plan followed. hBMSC were seeded on the PCL scaffolds and cultured under standard expansion conditions for 2 weeks; at day 14, hBMSC–PCL constructs were transferred to non-perfused/perfused bioreactors and exposed to chondrogenic induction conditions for 3 weeks. B) Representative images and culture conditions scheme (hypoxic environment 5%O_2/continuous flow rate of 0.2 mL min^{-1}) for the perfused culture of hBMSC–PCL constructs. C) Cell metabolic activity throughout culture. D) Metabolic analyses throughout culture expressed by the concentration profiles (in mM) for glucose (i) and lactate (ii). Note that the initial glucose concentration of expansion medium is 1.0 g L^{-1} while for the chondrogenic differentiation medium is ≈4.0 g L^{-1}. Results for cell numbers in non-perfused/perfused constructs are represented as mean ± SEM of three ($n = 3$) independent experiments.

Alcian Blue (**Figure 4**A), confirming the presence of sGAG. However, as shown in Figure 4B, perfused constructs presented a significantly higher ($p < 0.05$) amount of sGAG (19.0 ± 2.47 µg per scaffold) compared to constructs cultured without perfusion (10.62 ± 2.10 µg per scaffold). This observation suggests a beneficial effect of perfusion culture in promoting sGAG production by cells, resulting in an ≈1.8-fold increase compared to non-perfused constructs.

The final constructs were also processed and evaluated by histological (Figure 4C) and immunohistochemical analysis (Figure 4D). Both non-perfused/perfused constructs showed the presence of cells with defined nuclei after H&E staining (Figure 4C(i,ii)). Additionally, Toluidine Blue (Figure 4C(iii,iv)) and Safranin-O (Figure 4C(v,vi)) positive stainings for both conditions confirmed the presence of proteoglycans and GAG, respectively. Importantly, the apparently more intensive staining observed in Figure 4C(iv) and Figure 4C(vi) is consistent with the higher sGAG content (Figure 4B) observed for constructs obtained after perfusion bioreactor culture. Figure 4D shows the images resultant from the immunodetection protocol performed on the final constructs to assess for the presence of main cartilage ECM components, collagen II (Figure 4D(i,ii)) and aggrecan (Figure 4D(iii,iv)). While bioreactor culture under static conditions (Figure 4D(i)) and perfusion bioreactor culture (Figure 4D(ii)) lead to constructs staining positive for the presence of collagen II, the same was not observed for aggrecan. Perfused constructs showed more abundant and distributed positive staining for aggrecan (Figure 4D(iii)), in contrast to the small spots of lower aggrecan expression (highlighted by the black arrows) verified for the non-perfusion condition (Figure 4D(iv)). The higher aggrecan expression observed after perfusion culture is in agreement with the results presented above for sGAG amounts and histological analysis.

3.5. Flow Perfusion Promotes the Expression of Chondrogenic Genes While Reducing Hypertrophy

qPCR analysis was performed to assess the effects of the perfusion culture in the chondrogenic gene expression profile of

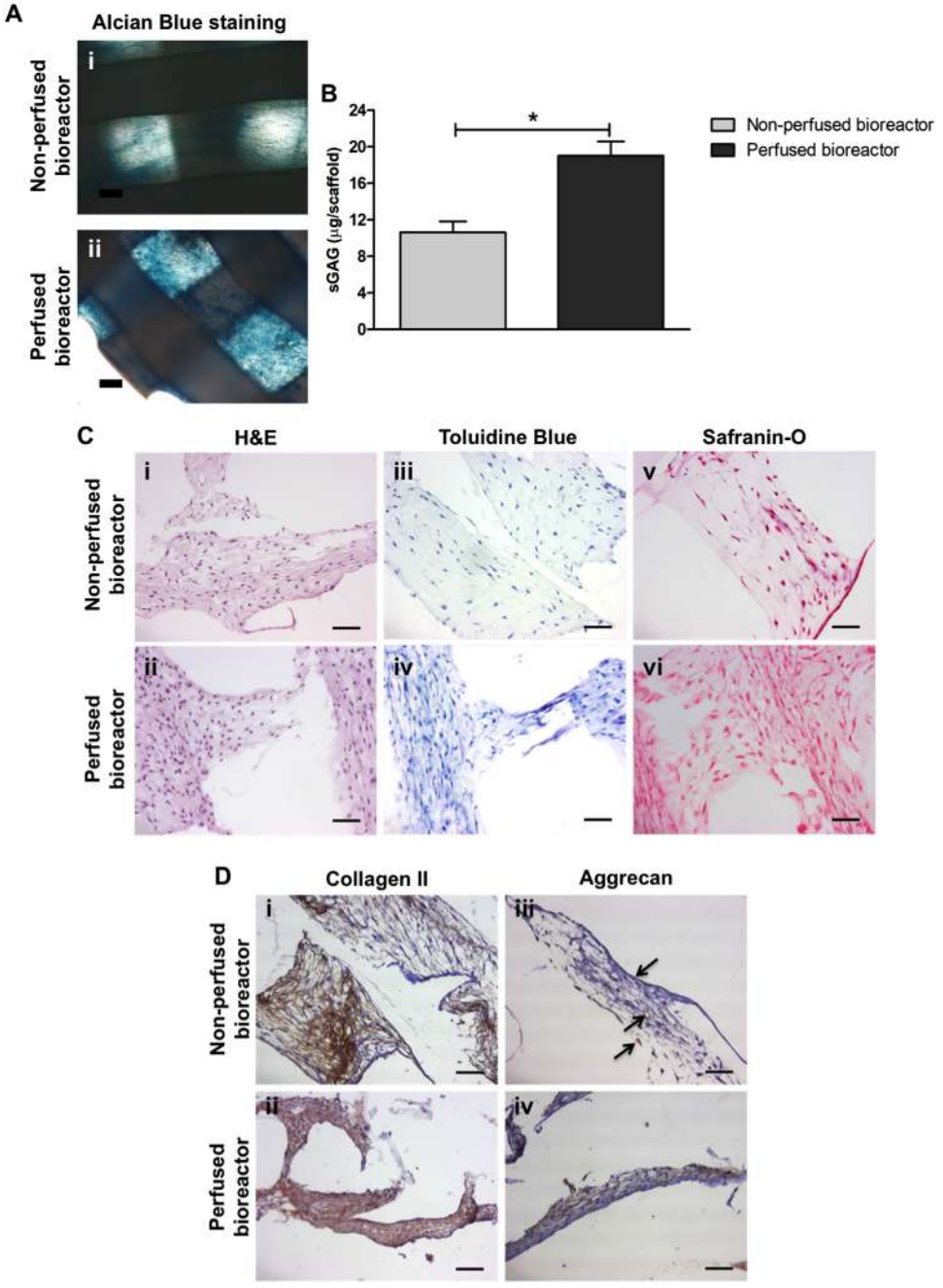

Figure 4. Perfused bioreactor culture of hBMSC–PCL constructs promotes cartilage ECM production. A) Alcian Blue staining in the final hBMSC–PCL constructs detect sGAG deposition after static (i) or perfusion (ii) bioreactor culture. Scale bar: 100 μm. B) Quantification of the amount of sGAG per scaffold obtained after non-perfused/perfused bioreactor culture. Results are expressed as mean ± SEM of three ($n = 3$) independent experiments. $^{*}p < 0.05$. C) Histological analysis of the final tissue constructs generated after static/perfused bioreactor culture: H&E (i, ii), Toluidine Blue (iii, iv), and Safranin-O (v, vi) staining. Scale bar: 50 μm. D) Immunohistochemical analysis of the final tissue constructs to detect main cartilage ECM components collagen II (static bioreactor (i) and perfusion bioreactor (ii)) and aggrecan (static bioreactor (iii) and perfusion bioreactor (iv)). Positive staining is observed in brown and samples were counterstained with haematoxylin. Black arrows highlight small spots of aggrecan expression. Scale bar: 50 μm.

the final constructs. RNA was isolated before scaffold seeding (day 0) and from constructs harvested after bioreactor culture under non-perfusion/perfusion conditions (day 35). **Figure 5** shows the values for gene expression of chondrogenic markers *Sox9* (Figure 5A), *ACAN* (Figure 5C), *COL II* (Figure 5E), fibrocartilage marker *COL I* (Figure 5B), hypertrophy marker *COL X* (Figure 5D), and osteogenic marker *Runx2* (Figure 5E), normalized to the housekeeping gene *GAPDH* expression and presented as fold-change relative to the values obtained for hBMSC at day 0. Perfused constructs presented significantly higher ($p < 0.05$)

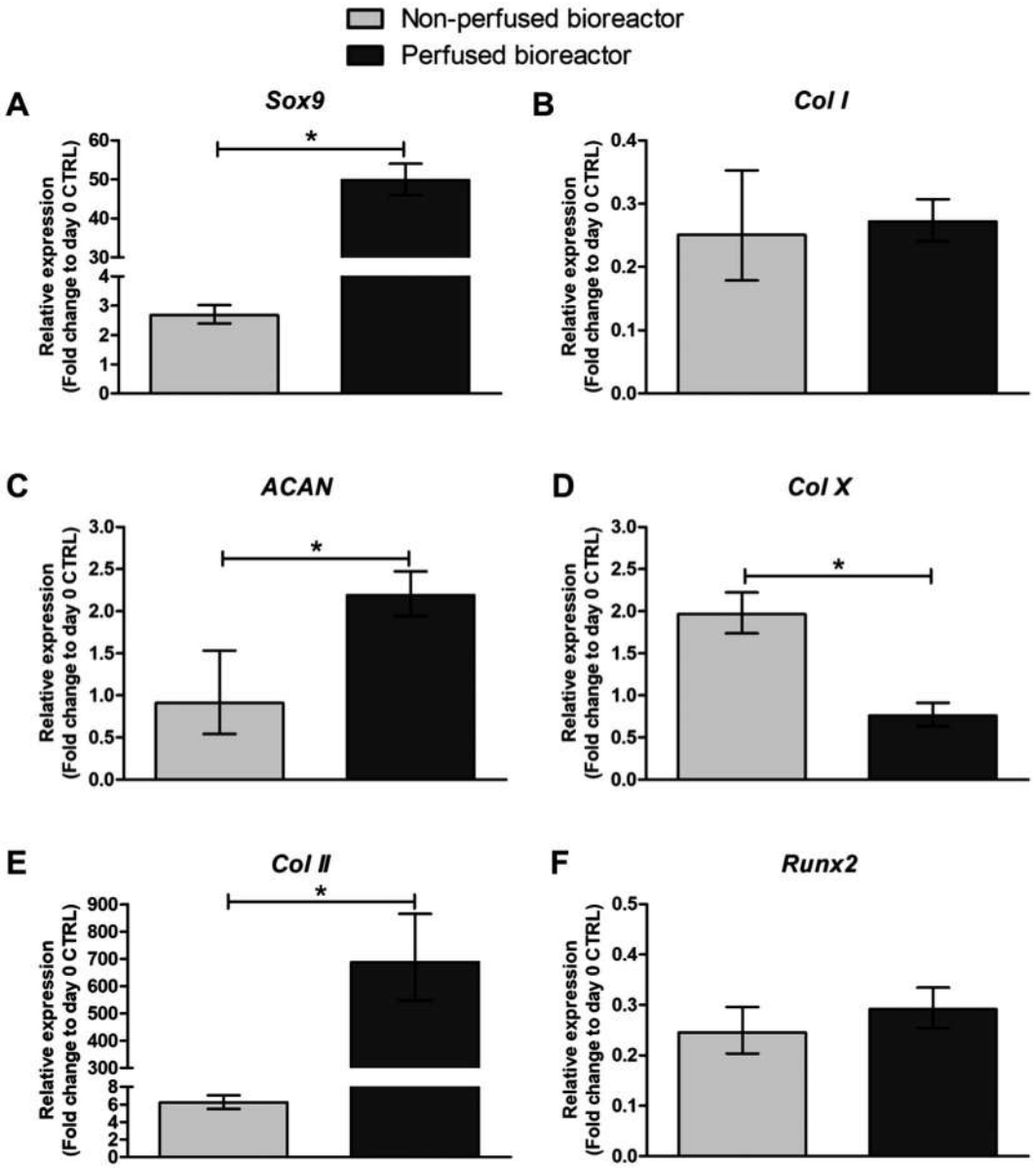

Figure 5. Gene expression evaluation by qPCR analysis of the final tissue constructs obtained after non-perfused/perfused bioreactor culture. A) *Sox9*, B) *Col I* (collagen type I), C) *ACAN* (aggrecan), D) *Col X* (collagen type X), E) *Col II* (collagen type II), and F) *Runx2* gene expressions are normalized against the housekeeping gene *GAPDH* and presented as fold-change levels relative to hBMSC at day 0 prior to scaffold seeding. Values are represented as mean ± SEM of three ($n = 3$) independent experiments. $^{*}p < 0.05$.

expression of chondrogenic markers *Sox9*, *ACAN*, and *COL II* compared to constructs cultured without perfusion. Such enhancement was considerably more pronounced for the expression of the main chondrocyte marker *COL II*. Regarding the expression of *COL I* and *Runx2*, both conditions showed down-regulation relative to hBMSCs at day 0 and no statistical differences were observed. Notably, the perfusion bioreactor platform developed here operating with a flow rate of 0.2 mL min^{-1} resulted in a statistically significant decrease ($p < 0.05$) in the expression of the hypertrophic marker *COL X* when compared to bioreactor culture under static conditions. Thus, our qPCR results suggest that perfused bioreactor culture of hBMSC–PCL constructs favored MSC chondrogenic differentiation while preventing tissue hypertrophy observed for non-perfused constructs.

4. Discussion

The role of mechanical signals in the regulation of MSC fate has been demonstrated and explored for a broad range of tissue engineering strategies.[54,55] In CTE, mechanical stimuli such as fluid flow-induced shear stress, compression, tension, and hydrostatic pressure have been applied alone or combined using bioreactor systems and demonstrated to promote the chondrogenic

potential of MSC.[22,29,30,33–36,56,57] However, the molecular mechanisms involved in the MSC mechanotransduction signaling are not fully understood.[58] Flow perfusion has been applied for the production of both MSC-based tissue-engineered bone[39,59] and cartilage.[32,33,60] Different magnitudes of shear stress generated by fluid perfusion have been reported to result in distinct engineered cartilage phenotypes.[34,56] Therefore, more studies on the effects of fluid perfusion on MSC chondrogenic differentiation are needed to deepen our understanding of the underlying molecular signaling involved and to define boundary stimulation conditions for magnitudes and regimes envisaging improved protocols for CTE approaches.

Bioreactors used to provide different mechanical stimuli in CTE are often complex systems designed to meet the requirements for a standardized scaffold size and architecture. Recently, AM technologies, which revolutionized the tissue engineering field by making possible the development of anatomically complex patient-customized implants, were also used for the manufacturing of versatile and cost-effective bioreactor platforms that can be easily modified according to the specificities of the target application.[37,39,61] The possibility of fabricating both scaffold and bioreactor devices with a high degree of customization and process automation is a critical step toward the efficient, fast, and reproducible production of personalized high-quality tissue substitutes.

In the present work, we used CAD and 3D extrusion to manufacture a custom-made bioreactor platform that allows study the effect of fluid perfusion on the chondrogenic differentiation of MSC in 3D porous PCL scaffolds, also fabricated by extrusion. CFD has been described as an invaluable tool to predict and visualize the distribution of fluidic velocities and forces within a bioreactor system, enabling a better understanding of the role of the hydrodynamic environment in tissue engineering strategies.[62] Herein, we performed a CFD analysis to predict fluid velocities distribution and intensity in different regions of the bioreactor to avoid any detrimental effects on the cells caused by shear stresses too high or by insufficient nutrient transfer. Additionally, our analysis predicted a homogeneous fluid perfusion in the regions tangential to the scaffolds, suggesting that all six scaffolds within the bioreactor would be exposed to similar hydrodynamic conditions. Prior to in vitro cell culture experiments, ABS material used to fabricate the bioreactor was tested for different printing infill following the ISO 10 993–5 guidelines and demonstrated high biocompatibility, which is in accordance with previously published literature on the use of ABS as scaffold for CTE.[63]

Similar to other studies focusing on chondrogenic differentiation,[64] we promoted an expansion phase to allow hBMSC growth and spreading throughout the PCL scaffolds, and afterwards, hBMSC–PCL constructs were transferred to perfusion bioreactor for mechanical stimulation. No statistical differences were observed in cell metabolic activities between perfused and non-perfused bioreactor culture, confirming that the flow rate selected did not cause any detrimental effect on cell viability and proliferation. The results reported by Tiğli et al.[64] were in agreement as no significant differences in cell proliferation were observed between non-perfusion and perfusion culture of human embryonic stem cell-derived MSC in porous silk scaffolds under chondrogenic induction. Additionally, Alves da Silva and colleagues[65] reported no differences in cell proliferation between static and perfused culture of PCL nanofiber meshes seeded with hBMSCs, during 21 days under chondrogenic differentiation conditions.

Our metabolite analysis, performed both during hBMSCs static expansion in PCL scaffolds placed in TCPS plates and chondrogenic differentiation in the bioreactor under static conditions or perfusion, revealed that exhaustion of glucose was never observed during the culture. Moreover, inhibitory lactate concentrations for MSCs over 35 mM[53] were never reached throughout all culture period, indicating that the media change protocol used was sufficient. Our results for glucose consumption/lactate production rates indicate a higher MSC energy metabolism during expansion with a considerable reduction during chondrogenesis, which is in agreement with the results reported by Pattappa et al. for pellet chondrogenic cultures.[66] Moreover, Gupta and colleagues also observed a decrease in glucose consumption and lactate production during chondrogenic differentiation of human periosteum-derived progenitor cells in spinner flasks.[26] MSCs have a metabolic requirement dominated by aerobic glycolysis during self-renewal, while upon differentiation, the metabolism shifts to oxidative phosphorylation.[67,68] We observed apparent yields of lactate from glucose >2 under both culture conditions, suggesting that lactate is being generated from alternative carbon sources, such as glutamine.[69]

Fluid perfusion in the bioreactor system produces shear stress that was previously shown to influence MSC differentiation processes.[54,70] Shear stress is known to activate MAPK signaling, which regulates both MSC osteogenic and chondrogenic differentiation.[71,72] At the end of the experiment, perfused constructs showed statistically significant higher sGAG amounts than the values obtained in non-perfusion culture, suggesting a favorable effect of flow perfusion in the production of cartilage ECM. This was also suggested by histological and immunohistochemical analysis of the final tissue constructs, mainly by the evidence of considerable higher expression and distribution of main cartilage constituent aggrecan after perfusion bioreactor culture, which is in accordance with the increased sGAG amounts and the more intense Toluidine Blue and Safranin-O staining. Our histological/immunohistochemical analysis data is in agreement with previous studies on the effect of perfusion culture in MSC chondrogenesis in CTE scaffolds.[60,65] Despite some authors reporting detrimental effects in sGAG production after perfusion culture,[32,34] others showed significantly higher amounts in perfused constructs,[64] which is in agreement with our results.

Gene expression results, namely the significantly higher expression levels of *Sox9*, *ACAN*, and *COL II* compared to non-perfused culture, as well as downregulation of *Runx2* and *COL I*, indicate that the flow perfusion culture protocol, using the bioreactor developed here, promotes MSC chondrogenic differentiation in 3D porous PCL scaffolds. Additionally, the perfused constructs presented significantly lower *COL X* expression than the non-perfused counterparts, suggesting a role of flow-induced shear stress in preventing tissue hypertrophy. A previous study using a perfusion bioreactor with a flow rate of 1 mL min^{-1} to promote chondrogenesis, showed similar trends for cartilage marker genes, however, data on *COL X* expression were not provided.[64] Interestingly, other authors

reported decreased expression of the hypertrophic marker *COL X* in chitosan-based scaffolds cultured with hBMSC in a perfusion bioreactor, in comparison to the constructs maintained without perfusion.[60]

MSC differentiation fate regulation through perfusion has also been predicted to be dependent on the flow rate magnitudes involved.[56] While there are studies reporting the positive effect of fluid perfusion in MSC chondrogenic differentiation on tissue engineering scaffolds,[33,64] others have demonstrated detrimental effects such as tissue hypertrophy, reduced GAG production, and lower cell viabilities.[32,34] Nevertheless, two recent studies highlighting the rate of fluid shear stress as an effective regulator of the chondrogenic differentiation of MSC in 2D culture conditions,[73,74] suggest that when using 3D scaffolds systems, different flow rate magnitudes might also result in different outcomes. In the current study, a mild perfusion flow rate of 0.2 mL min^{-1} was selected to provide uniform linear fluid velocities along the scaffold, resulting in an interesting enhancement of the hBMSC chondrogenic potential and reduced hypertrophy, in comparison to the non-perfused condition. Nevertheless, when making comparisons, it is important to consider the differences in bioreactor platform geometry and flow rate magnitudes/regimes used in each study and to note that distinct MSC chondrogenic differentiation outputs might arise not only from the perfusion effect but also from the type of MSC-source (e.g., BMSC, synovium-derived MSC, adipose tissue-derived MSC, umbilical cord blood-derived MSC), the scaffold material/structure as well as from the culture media/protocol used.

In conclusion, we present a unique concept of a fully customizable, AM-based extrusion, perfusion bioreactor, capable of providing flow-induced shear stress stimuli to MSC-based tissue constructs for CTE applications. Our results demonstrate that a perfusion bioreactor culture promotes the chondrogenic differentiation of hBMSCs, as suggested by increased cartilage-like ECM production and expression of chondrogenic marker genes when compared to non-perfusion culture conditions. In this first proof-of-concept study, we performed our in vitro culture experiments under a single flow rate. A study varying flow rate stimulation values and using a Design of Experiments strategy should be performed to determine the optimal perfusion bioreactor operating conditions required to maximize the chondrogenic potential of MSC, assessed in vitro. Considering previous studies reporting enhanced expression of chondrogenic markers by MSC-based constructs cultured under perfusion in basal media,[75] it would be interesting to further use our perfusion bioreactor platform to investigate MSC fate in the absence of chondrogenic induction medium. Additionally, the versatility of the platform presented here allows tailoring scaffolds to different types of 3D culture systems such as cell pellets or micromasses. Therefore, the study of the effect of cell culture technique (i.e., a comparison between MSCs seeded on scaffolds and MSC pellets assembled in scaffolds) on MSC chondrogenic differentiation under perfusion conditions is particularly interesting and should be addressed in the future. As articular cartilage motion results from a combination of compressive, tensile. and shear stresses,[35] future studies should also focus on the development of novel AM-based bioreactor platforms enabling the application of multiple mechanical stimuli simultaneously to enhance MSC chondrogenesis by providing a closer mimicry of the native cartilage microenvironment. Such bioreactor platforms should be further customized to integrate different combinations of scaffold materials and structures such as hydrogels or electrospun fibers that are required to mimic the hierarchical multizonal structure of the articular cartilage tissue. Also, the application of different mechanical stimuli to tissue constructs produced in scaffolds with varying properties such as stiffness, internal architecture. and porosity would provide a better understanding of how these scaffold features affect MSC mechanotransduction signals toward a chondrocyte-like phenotype.

The work here described presents a promising bioreactor platform for personalized CTE strategies and in vitro disease modeling while highlighting the advantages of AM-based bioreactor development for the automated fabrication of patient-tailored tissue engineering products targeting a wide range of regenerative medicine applications.

Supporting Information

Supporting Information is available from the Wiley Online Library or from the author.

Acknowledgements

The authors acknowledge financial support from Fundação para a Ciência e Tecnologia (FCT, Portugal) through UID/BIO/04565/2019, UID/Multi/04044/2013), Stimuli2BioScaffold grant (PTDC/EMESIS/32554/2017), and scholarships SFRH/BD/73970/2010, SFRH/BD/105771/2014, and SFRH/BSAB/128442/2017. Funding from Programa Operacional Regional de Lisboa 2020 (project no. 007317) and also through the projects PRECISE (PAC-PRECISE-LISBOA-01-0145-FEDER – 016394, SAICTPAC/0021/2015) and POCI-01-0145-FEDER-016800 is also acknowledged.

Conflict of Interest

The authors declare no conflict of interest.

Keywords

additive manufacturing, cartilage tissue engineering, extrusion-based perfusion bioreactor, mesenchymal stem/stromal cells, poly(ε-caprolactone) scaffolds

Received: March 2, 2019
Revised: September 9, 2019
Published online:

[1] B. J. Huang, J. C. Hu, K. A. Athanasiou, *Biomaterials* **2016**, *98*, 1.
[2] A. R. Tan, C. T. Hung, *Stem Cells Transl. Med.* **2017**, *6*, 1295.
[3] C. Madeira, A. Santhagunam, J. B. Salgueiro, J. M. S. Cabral, *Trends Biotechnol.* **2015**, *33*, 35.

[4] J. C. Bernard, G. Vunjak-Novakovic, *Stem Cell Res. Ther.* **2016**, *7*, 56.
[5] C. Vinatier, D. Murgala, C. Jorgensen, J. Guicheux, D. Noël, *Trends Biotechnol.* **2009**, *27*, 307.
[6] M. F. Pittenger, A. M. Mackay, S. C. Beck, R. K. Jaiswal, R. Douglas, J. D. Mosca, M. A. Moorman, D. W. Simonetti, S. Craig, D. R. Marshak, *Science* **1999**, *284*, 143.
[7] G. Chamberlain, J. Fox, B. Ashton, J. Middleton, *Stem Cells* **2007**, *25*, 2739.
[8] S. Camarero-Espinosa, B. Rothen-Rutishauser, E. J. Foster, C. Weder, *Biomater. Sci.* **2016**, *4*, 734.
[9] D. Puppi, F. Chiellini, A. M. Piras, E. Chiellini, *Prog. Polym. Sci.* **2010**, *35*, 403.
[10] W. J. Li, R. Tuli, C. Okafor, A. Derfoul, K. G. Danielson, D. J. Hall, R. S. Tuan, *Biomaterials* **2005**, *26*, 599.
[11] H. J. Kim, J. H. Lee, G. I. Im, *J. Biomed. Mater. Res.Part A* **2010**, *92*, 659.
[12] K. Theodoridis, E. Aggelidou, T. Vavilis, M. E. Manthou, A. Tsimponis, E. C. Demiri, A. Boukla, C. Salpistis, A. Bakopoulou, A. Mihailidis, A. Kritis, *J. Tissue Eng. Regener. Med.* **2019**, *13*, 342.
[13] S. van Uden, J. Silva-Correia, V. M. Correlo, J. M. Oliveira, R. L. Reis, *Biofabrication* **2015**, *7*, 015008.
[14] A. S. Htay, S. H. Teoh, D. W. Hutmacher, *J. Biomater. Sci., Polym. Ed.* **2004**, *15*, 683.
[15] R. L. Mauck, S. B. Nicoll, S. L. Seyhan, G. A. Ateshian, C. T. Hung, *Tissue Eng.* **2003**, *9*, 597.
[16] E. Mariani, L. Pulsatelli, A. Facchini, *Int. J. Mol. Sci.* **2014**, *15*, 8667.
[17] G. Cai, W. Liu, Y. He, J. Huang, L. Duan, J. Xong, L. Liu, D. Wang, *J. Drug Targeting* **2019**, *27*, 28.
[18] S. Zhou, Z. Cui, J. P. G. Urban, *Arthritis Rheum.* **2004**, *50*, 3915.
[19] P. H. Oliveira, J. S. Boura, M. M. Abecassis, J. M. Gimble, C. L. da Silva, J. M. S. Cabral, *Stem Cell Res.* **2012**, *9*, 225.
[20] J. Leijten, N. Georgi, L. Moreira Teixeira, C. A. van Blitterswijk, J. M. Post, M. Karperien, *Proc. Natl. Acad. Sci. U. S. A.* **2014**, *111*, 13954.
[21] J. J. Vaca-González, J. M. Guevara, M. A. Moncayo, H. Castro-Abril, Y. Hata, D. A. Garzón-Alvarado, *Cartilage* **2019**, *10*, 157.
[22] K. Li, C. Zhang, L. Qiu, L. Gao, X. Zhang, *Tissue Eng., Part B* **2017**, *23*, 399.
[23] T. D. Bornes, N. M. Jomha, A. Mulet-Sierra, A. B. Adesida, *Stem Cell Res. Ther.* **2015**, *6*, 84.
[24] C. Gaut, K. Sugaya, *Regener. Med.* **2015**, *10*, 665.
[25] F. Dos Santos, A. Campbell, A. Fernandes-Platzgummer, P. Z. Andrade, J. M. Gimble, Y. Wen, S. Boucher, M. C. Vemuri, C. L. da Silva, J. M. S. Cabral, *Biotechnol. Bioeng.* **2014**, *111*, 1116.
[26] P. Gupta, L. Geris, F. P. Luyten, I. Papantoniou, *Biotechnol. J.* **2018**, *13*, 1700087.
[27] J. Hansmann, F. Groeber, A. Kahlig, C. Kleinhans, H. Walles, *Biotechnol. J.* **2013**, *8*, 298.
[28] L. Bian, D. Y. Zhai, E. C. Zhang, R. L. Mauck, J. A. Burdick, *Tissue Eng., Part A* **2012**, *18*, 715.
[29] A. H. Huang, M. J. Farrell, M. Kim, R. L. Mauck, *Eur. Cells Mater.* **2010**, *19*, 72.
[30] C. Correia, A. L. Pereira, A. R. C. Duarte, A. M. Frias, A. J. Pedro, J. T. Oliveira, R. A. Sousa, R. L. Reis, *Tissue Eng., Part A* **2012**, *18*, 1979.
[31] Z. Li, S.-J. Yao, M. Alini, M. J. Stoddart, *Tissue Eng., Part A* **2010**, *16*, 575.
[32] A. Gonçalves, P. Costa, M. T. Rodrigues, I. R. Dias, R. L. Reis, M. E. Gomes, *Acta Biomater.* **2011**, *7*, 1644.
[33] N. Mahmoudifar, P. M. Doran, *Biomaterials* **2010**, *31*, 3858.
[34] L. M. Kock, J. Malda, W. J. A. Dhert, K. Ito, D. Gawlitta, *J. Biomech.* **2014**, *47*, 2122.
[35] O. Schätti, S. Grad, J. Goldhahn, G. Salzmann, Z. Li, M. Alini, M. J. Stoddart, *Eur. Cells Mater.* **2011**, *22*, 214.
[36] C. Meinert, K. Schrobback, D. W. Hutmacher, T. J. Klein, *Sci. Rep.* **2017**, *7*, 16997.
[37] P. F. Costa, C. Vaquette, J. Baldwin, M. Chhaya, M. E. Gomes, R. L. Reis, C. Theodoropoulos, D. W. Hutmacher, *Biofabrication* **2014**, *6*, 035006.
[38] I. Martin, T. Smith, D. Wendt, *Trends Biotechnol.* **2009**, *27*, 495.
[39] C. Mota, D. Puppi, F. Chiellini, E. Chiellini, *J. Tissue Eng. Regener. Med.* **2015**, *9*, 174.
[40] M. J. Jaasma, N. A. Plunkett, F. J. O'Brien, *J. Biotechnol.* **2008**, *133*, 490.
[41] F. Dos Santos, P. Z. Andrade, J. S. Boura, M. M. Abecasis, C. L. da Silva, J. M. S. Cabral, *J. Cell. Physiol.* **2010**, *223*, 27.
[42] M. Domingos, D. Dinucci, S. Cometa, M. Alderighi, P. J. Bártolo, F. Chiellini, *Int. J. Biomater.* **2009**, 239643.
[43] J. C. Silva, C. S. Moura, N. Alves, J. M. S. Cabral, F. C. Ferreira, *Procedia Manuf.* **2017**, *12*, 132.
[44] ISO 10993-5, Biological evaluation of medical devices Part 5: Tests for in vitro cytotoxicity **2009**.
[45] C. S. Moura, C. L. da Silva, P. J. Bártolo, F. C. Ferreira, *Proc. Eng.* **2015**, *110*, 122.
[46] N. Mahmoudifar, P. M. Doran, *Biotechnol. Bioeng.* **2005**, *91*, 338.
[47] J. T. Dingle, P. Horsfield, H. B. Fell, M. E. J. Barratt, *Ann. Rheum. Dis.* **1975**, *34*, 303.
[48] J. Nam, J. Johnson, J. J. Lannutti, S. Agarwal, *Acta Biomater.* **2011**, *7*, 1516.
[49] A. Matsiko, J. P. Gleeson, F. J. O'Brien, *Tissue Eng., Part A* **2015**, *21*, 486.
[50] Y. Zhao, K. Tan, Y. Zhou, Z. Ye, W.-S. Tan, *Mater. Sci. Eng., C* **2016**, *59*, 193.
[51] S. S. Stevens, G. S. Beaupré, D. R. Carter, *J. Orthop. Res.* **1999**, *17*, 646.
[52] D. R. Carter, M. Wong, *Philos. Trans. R. Soc. Lond. Ser. B Biol. Sci.* **2003**, *358*, 1461.
[53] D. Schop, F. W. Janssen, L. D. S. van Rijn, H. Fernandes, R. M. Bloem, J. D. de Bruijn, R. van Dijkhuizen-Radersma, *Tissue Eng., Part A* **2009**, *15*, 1877.
[54] D. J. Kelly, C. R. Jacobs, *Birth Defects Res. Part C* **2010**, *90*, 75.
[55] J. Hao, Y. Zhang, D. Jing, Y. Shen, G. Tang, S. Huang, Z. Zhao, *Acta Biomater.* **2015**, *20*, 1.
[56] E. Y. Salinas, J. C. Hu, K. A. Athanasiou, *Tissue Eng., Part B* **2018**, *24*, 345.
[57] N. Fahy, M. Alini, M. J. Stoddart, *J. Orthop. Res.* **2018**, *36*, 52.
[58] J. A. Panadero, S. Lanceros-Mendez, J. L. G. Ribelles, *Acta Biomater.* **2016**, *33*, 1.
[59] G. Chen, R. Xu, C. Zhang, Y. Lv, *ACS Appl. Mater. Interfaces* **2017**, *9*, 1207.
[60] M. L. Alves da Silva, A. Martins, A. R. Costa-Pinto, V. M. Correlo, P. Sol, M. Bhattacharya, S. Faria, R. L. Reis, N. M. Neves, *J. Tissue Eng. Regener. Med.* **2011**, *5*, 722.
[61] P. F. Costa, D. W. Hutmacher, C. Theodoropoulos, M. E. Gomes, R. L. Reis, C. Vaquette, *Adv. Healthcare Mater.* **2015**, *4*, 864.
[62] D. W. Hutmacher, H. Singh, *Trends Biotechnol.* **2008**, *26*, 166.
[63] D. H. Rosenzweig, E. Carelli, T. Steffen, P. Jarzem, L. Haglund, *Int. J. Mol. Sci.* **2015**, *16*, 15118.
[64] R. S. Tiğli, C. Cannizaro, M. Gümüşderelioğlu, D. L. Kaplan, *J. Biomed. Mater. Res., Part A* **2011**, *96A*, 21.
[65] M. L. Alves Da Silva, A. Martins, A. R. Costa-Pinto, P. F. Costa, S. Faria, M. E. Gomes, R. L. Reis, N. M. Neves, *Biomacromolecules* **2010**, *11*, 3228.
[66] G. Pattappa, H. K. Heywood, J. D. de Bruijn, D. A. Lee, *J. Cell. Physiol.* **2011**, *226*, 2562.

[67] C. D. L. Folmes, P. P. Dzeja, T. J. Nelson, A. Terzic, *Cell Stem Cell* **2012**, *11*, 596.
[68] M. Liu, Y. Li, S. T. Yang, *Biochem. Eng. J.* **2014**, *82*, 71.
[69] G. Eibes, F. dos Santos, P. Z. Andrade, J. S. Boura, M. M. Abecasis, C. L. da Silva, J. M. S. Cabral, *J. Biotechnol.* **2010**, *146*, 194.
[70] A. B. Yeatts, D. T. Choquette, J. P. Fisher, *Biochim. Biophys. Acta, Gen. Subj.* **2013**, *1830*, 2470.
[71] G. Yourek, S. M. McCormick, J. J. Mao, G. C. Reilly, *Regener. Med.* **2010**, *5*, 713.
[72] J. B. Fitzgerald, M. Jin, D. H. Chai, P. Siparsky, P. Fanning, A. J. Grodzinsky, *J. Biol. Chem.* **2008**, *283*, 6735.
[73] J. Lu, Y. Fan, X. Gong, X. Zhou, Y. Caixia, Y. Zhang, J. Pan, *J. Cell. Physiol.* **2016**, *231*, 1752.
[74] D. Yue, M. Zhang, J. Lu, J. Zhou, Y. Bai, J. Pan, *J. Cell. Physiol.* **2019**, *234*, 16312.
[75] W. Baumgartner, L. Otto, S. C. Hess, W. J. Stark, S. Märsmann, G. M. Bürgisser, M. Calcagni, P. Cinelli, J. Buschmann, *J. Biomed. Mater. Res., Part B* **2019**, *107*, 1833.